Analysis of Sample Acquisition Dynamics Using Discrete Element Method

Damiana Catanoso
USRA
NASA Ames Research Center
Moffett Field, CA 94035
damiana.catanoso@nasa.gov

Thomas Stucky
SETI Institute
189 Bernardo Ave, Suite 200
Mountain View, CA 94043
tstucky@seti.org

Jennifer Case
NSTRF
Purdue University
West Lafayette, IN 47907
case15@purdue.edu

Arno Rogg
KBR
NASA Ames Research Center
Moffett Field, CA 94035
arno.rogg@nasa.gov

Abstract— **The analysis presented in this paper is conducted in the framework of the Ocean Worlds Autonomy Testbed for Exploration Research and Simulation (OceanWATERS) project, currently under development at NASA Ames Research Center. OceanWATERS aims at designing a simulation environment which allows for testing autonomy of scientific lander missions to the icy moons of our solar system. Mainly focused on reproducing the end effector interaction with the inherent terrain, this paper introduces a novel discrete element method (DEM)-based approach to determine forces and torques acting on the lander's scoop during the sample acquisition process. An accurate force feedback from the terrain on the scoop is required by fault-detection and autonomous decision-making algorithms to identify when the requested torque on the robotic arm's joints exceeds the maximum available torque. Knowledge of the terrain force feedback significantly helps evaluating the arm's links structural properties and properly selecting actuators for the joints. Models available in literature constitute a partial representation of the dynamics of the interaction. As an example, Balovnev derived an analytical expression of the vertical and horizontal force acting on a bucket while collecting a sample as a function of its geometry and velocity, soil parameters and reached depth. Although the model represents an adequate approximation of the two force components, it ignores the direction orthogonal to the scoop motion and neglects the torque. This work relies on DEM analysis to compensate for analytical models' deficiencies and inaccuracies, i. e. provide force and torque 3D vectors, defined in the moving reference (body) frame attached to the scoop, at each instant of the sample collection process. Results from the first presented analysis relate to the specific OceanWATERS sampling strategy, which consists of collecting the sample through five consecutive passes with increasing depth, each pass following the same circular-linear-circular trajectory. Data is collected given a specific scoop design interacting with two types of bulk materials, which may characterize the surface of icy planetary bodies: snow and ice. Although specifically concerned with the OceanWATERS design, this first analysis provides the expected force trends for similar sampling strategies and allows to deduce phenomenological information about the general scooping process. In order to further instruct the community on the use of DEM tools as a solution to the sampling collection problem, two more analyses have been carried out, mainly focused on reducing the DEM computation time, which increases with a decrease in particle size. After running a set of identical simulations, where the only changing parameter is the size of the spherical particle, it is observed that the resulting force trajectories, starting from a given particle size, converge to the true trend. It is deducible that a further decrease in size yields negligible improvements in the accuracy, while it sensibly increases computation time. A final analysis aims at discussing limitations of approximating bulk material particles having a complex shape, e. g. ice fragments, with spheres, by comparing force trends resulting in the two cases for the same simulation scenario.**

TABLE OF CONTENTS

1. INTRODUCTION

Icy worlds have gained attention in the recent years for their environmental conditions suitable for the development of life. Multiple icy worlds are present in our solar system such as Enceladus and Europa, two moons orbiting around Saturn and Jupiter respectively [1]. Recently, the Cassini probe data revealed some organic molecules on Enceladus, reinforcing the theory of those worlds being suitable for life organisms development [2]. In order to test different autonomous science operations algorithms for future lander missions to icy worlds, NASA Ames Research Center is developing the Ocean Worlds Autonomy Testbed for Research and Simulation (OceanWATERS).

In parallel to the software simulation, the NASA Jet Propulsion Laboratory (JPL) is developing a physical testbed for simulation validation and testing. The JPL Europa Lander [3] has been chosen as reference mission for the software and hardware testbed development. However, applicability of OceanWATERS extends to all future missions landing on icy planets.

OceanWATERS is being developed leveraging the team's expertise on the Robotic Operating System (ROS) and Gazebo, acquired during the development of a simulation environment for the Resource Prospector (RP) Lunar rover project [4]. ROS is an open source robotics tool enabling the fast development of complex robotics systems. Gazebo, on the other hand, is a physical simulator used to provide the ROS-based simulated robotic systems with an environment to evolve in [5].

This paper focuses on the lander's robotic arm and, more specifically, the end effector to soil interaction. Previous NASA missions robotic systems interacted with soils on extraterrestrial bodies using an end effector. A non-exhaustive list includes: the Rock Abrasion Tool (RAT) from the Spirit and Opportunity Mars Exploration Rovers (MER) [6], the Sample Acquisition System from the Curiosity Mars Science Laboratory (MSL) [7], and the Icy Soil Acquisition Device (ISAD) from the Phoenix Lander [8]. The Phoenix ISAD is the closest end effector to the one presented in this paper. It has been used to dig, scrap and rasp the Mars dry and icy surfaces. The operation concept for this particular end effector was to use the scoop to trench loose ground over tens of centimeters and a dozen centimeters deep.

The paper presents collected numerical data on forces and torques applied to the scoop during a trenching motion through granular soil, simulated using a discrete element method (DEM) model. Two representative types of material (snow and ice fragments) are considered in this paper. However, the same DEM simulation can be run for different terrain types through changing the bulk material and interaction parameters. The scoop is digging through several passes at increasing depth. The forces and torques data resulting from the DEM simulation is then embedded in a lookup table included in the OceanWATERS Gazebo framework. Furthermore, this paper presents a survey of soil types possibly present on Europa, gathering information about the icy terrain properties to provide context for the soil parameter assumptions. Finally, the paper presents an optimization study of the different simulated parameters to reduce the DEM computation time.

Different approaches have been used in literature and previous projects to estimate excavation forces and torques in granular terrain. Common approaches consist of the adoption of analytical models, such as the Balovnev equations [9], empirical models, obtained by means of physical testbed, or discrete element method-based simulation at particle level. Although attractive for their simplicity, analytical models have several major limitations: they do not sufficiently distinguish between different scoop geometries, and they do not handle heterogeneous or more complex terrain structures. As for empirical models, their accuracy is limited to specific applications and scenarios that can physically be reproduced. They are well suited when parameters are known and do not change, while it results difficult to test over a broad variety of input parameters. Furthermore, challenges arise when environmental factors such as gravity and temperature are widely different than what is found on Earth [10]. Conversely, DEM-based methods take into account the specific end effector geometry, the soil property and the environmental conditions, providing a more realistic and customizable force feedback characterization. DEM models are based on the modeling of physical interactions at a particle level, taking into account elastic forces, normal and rolling friction, plastic deformation of the particles and cohesion [11]. DEM is popular in the mining industry, where the modeling of large-scale processes aids efficient design of excavation and material transportation machinery. One of the most popular DEM modeling and analysis tools is the commercial software EDEM, chosen for OceanWATERS because of its maturity and library of validated materials [12].

This paper is articulated in five sections. After this introduction, Section 2 presents an overview of the possible features of Europa's terrain and justifies the choices of the particle parameters used in the simulations. Section 3 presents the sample collection strategy adopted in this study and for the OceanWATERS simulation. Section 4 presents results of targeted analyses aimed at efficiently simulating the sample collection using DEM.

2. EUROPA TERRAIN CHARACTERIZATION

The solar system contains numerous confirmed (Europa, Enceladus, Ganymede [13]) and unconfirmed (Callisto, Pluto) icy ocean worlds. For the purpose of this study we focus on Europa, currently under the radar for future space missions. An early stage concept for a Europa lander mission is discussed in detail in [14], and was used as a reference for the types of activities a lander should be expected to perform on Europa. Included among these activities are terrain interaction: poking, digging or cutting of surface ice, and scooping of the resulting tailings. To simulate these activities using DEM, the chemical content and structure of the surface and subsurface of Europa should be understood.

Europa's surface temperature range between 76 and 132 K [15]. Jupiter's magnetosphere delivers a bombardment of heavy radiation to Europa's surface that plays a key role in its surface properties through a process known as sputtering. The moon is tidally locked with Jupiter, which results in subtle differences in surface characteristics between its trailing and leading hemispheres. The low number of craters implies it has a relatively young surface age, between 40-60 million years [16]; however, this smooth surface is broken up by cracks and sublimation-driven features, such as the penitentes, reaching heights of 15 meters in the equatorial region [17].

The surface consists primarily of water ice in one of three forms: low-density amorphous (LDA) ice, the familiar hexagonal crystalline ice ($I_a h$) seen on Earth, and hydrated materials. LDA ice is a special form of water ice that forms from water vapor under low pressure between 100 K and 140 K [15]. Amorphous ice deposits on the surface of Europa in the form of frost, then transitions into crystalline ice over the time span of only about 10 years [15]. Radiation on the topmost layers causes a reverse reaction to occur where crystalline ice transitions back into LDA ice. The two processes together establish an equilibrium between the two states, such that at a particular depth we expect the LDA ice to give way to crystalline ice. Data from the Near-Infrared Mapping Spectrometer (NIMS) aboard the Galileo space probe has been used to confirm this hypothesis. In [18], Hansen et. al. found that Europa's surface is coated in a thin dusting of LDA ice down to only as deep as 1 mm. Below this depth the ice content is primarily in crystalline or possibly a mixture of crystalline and LDA ice that is known as restrained amorphous ice (I_r). NIMS spectra have also revealed mixtures of water and other chemical species known as hydrates on the surface, with the trailing side containing a higher concentration than the leading side [18]. The ice-mixed compounds are either salt or sulfuric acid [18]. There are smaller concentrations of other chemical species, but their presence is unlikely to affect the material properties by an appreciable amount for the purpose of terrain interaction.

NIMS data suggests ice is deposited on Europa's surface boundary with a grain size between 20 and 50 μm [15]. Bonds between these grains can be formed and strengthened through a process known as sintering, whereby lattice diffusion and vapor transport work to maximize the contact area between neighboring grains [19]. The sintering timescale is

proportional to temperature, which is higher at the topmost surface layer than at deeper depths when averaged over the diurnal cycle. This would result in more sintered material near the surface, which would cause a decrease in material hardness with increased depth for shallow digs (i.e. within 1 m). On the other hand, sputtering, a process driven by the surface radiation, breaks up materials on the topmost surface layer. Depending on which of these process dominates (sputtering or sintering) the reverse gradient may be observed within 1 m, where hardness will increase with depth. Two additional edge cases can be considered: extremely sintered material and extremely sputtered material. Where in the case of extremely sintered material something approaching solid polycrystalline ice is expected, for extremely sputtered material we unbonded granular ice particles are more likely to exist.

Material Selection & Justification

Both theory and NIMS data suggest that hexagonal crystalline ice ($I_a h$) is an appropriate target material to simulate for terrain interaction on the surface of Europa. For the purpose of these simulations hexagonal ice will be simulated in two forms: snow and crushed ice. Snow approximates the case where surface ice, due to weak sintering and/or strong sputtering, is mostly unconsolidated and can be scooped without too much processing of the material. Crushed ice approximates the case where surface ice, due to strong sintering and/or weak sputtering, is strengthened enough to the point it needs to be processed with either a drill or some other cutting implement before scooping of the tailings may occur. The elastic properties and internal friction for both particle types were selected to be Earth-like hexagonal crystalline ice just under 273 K. Cohesion between particles is assumed to be negligible, the reason being that in the low pressure environment of Europa water will sublime instead of melt, so the liquid water surface tension that allows for cohesion between ice particles on Earth is not present. The snow particles were given a lower density to account for their greater porosity, and the crushed ice particles were simulated as both spheres and tetrahedrons approximated by multi-spheres meshes to simulate a jagged shape that can interlock. The material properties for both the snow and crushed ice particles that were simulated can be found in Table 6.

3. SAMPLE COLLECTION STRATEGY

For the study presented in this paper, a simplified version of the scoop design from the Phoenix Mars Lander has been adopted [20]. The simplified scoop and its body frame are shown in Figure 1. A sample collection strategy was developed and used in the OceanWATERS Gazebo framework. However, a specific study focused on optimizing the trajectory is yet to be conducted and may result in modifications of the given sampling approach. The sample collection strategy consists of a sequence of five passes of the scoop through the same terrain region digging deeper with each pass. Each pass is also called a bite. When one pass is over, the scoop is emptied, with the collected soil deposited in a safe zone, and the next pass is commenced. Between two consecutive bites, the excavated depth increases a fixed quantity, referred to as bite depth b_d from now on. At the end of the scooping maneuver the total excavated depth corresponds to $d = 5b_d$. This number was arbitrarily defined as a good trade off between number of simulations and trench final depth. All passes are characterized by the same scoop trajectory. Figure 2 shows the three main steps constituting the scoop motion, which are: 1) the scoop approaches and enters the soil through a rotation

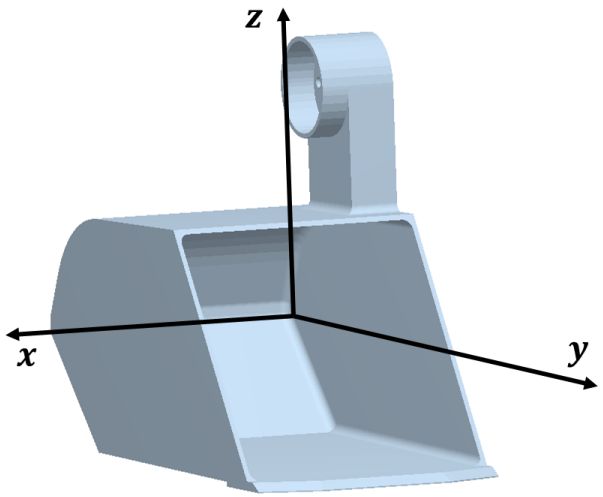

Figure 1. The scoop's body frame is centered on the center of mass of the scoop and having the X-axis parallel to the joint rotation axis, the Z-axis parallel and opposite to the gravity vector and the Y-axis obtained through the product Z×X. This is a digital replica of the Phoenix Mars Lander scoop, courtesy of NASA Jet Propulsion Laboratory.

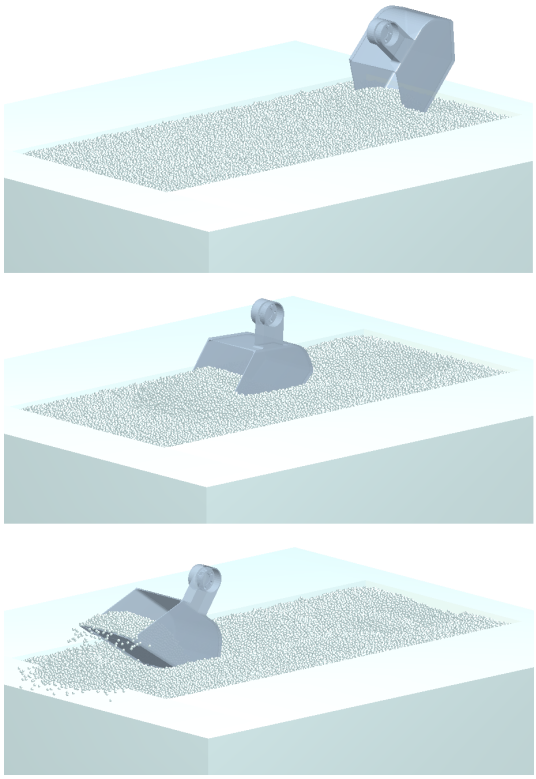

Figure 2. Capture of the DEM simulation. Top image shows the scoop entering the particle bed. Middle image shows the scoop traversing parallel to the surface. Bottom image shows the scoop exiting the granular material.

around its joint axis which ends with the scoop's blade parallel to the ground plane; 2) then, the scoop starts a linear motion parallel to the surface, traversing a few scoop lengths; 3) finally, the scoop performs a second rotation which ends the pass. For larger bite depths, the first contact with the terrain happens during the initial vertical approach, before the first rotation starts. In order to implement this sample collection strategy in the OceanWATERS Gazebo framework, force and torques on the scoop collected from simulations will be embedded in a lookup table which provides force feedback data for the scoop on demand. The Python function implemented in Gazebo is:

$$[F_x, F_y, F_z, T_x, T_y, T_z] = f(m, b_d, p, \rho). \quad (1)$$

The function takes in input: the material type (m), snow or ice; the bite depth, a float value between 0 and 15 mm; the pass number (p), a positive integer from 1 to 5; the relative distance covered along the trench since the first contact with the terrain (ρ), from 0 to 450 mm. The output consists of the three components of force and torque vectors in the scoop's body reference frame (Figure 1).

4. Simulation Methods & Results

This section shows results of the implementation of the scooping strategy described in the previous section in a discrete element method software. The simulations presented here have been run using the commercial software EDEM, developed by EDEM Solutions, installed on a Dell Desktop Computer with an Intel(R) i7 Xeon(R) W-2133 processor and 3.60 GHz CPU with 6 Cores and 8.25 MB cache. The graphics card is Nvidia Quadro P4000 8 GB. EDEM used a combination of 4 CPU cores and the GPU.

To analyze the forces and torques on the scoop, DEM software breaks solid geometries into some number of facets and calculates the force vector, resulting from the soil-geometry interaction, on each facet. These facet forces can then be summed to find the force vector on the whole geometry (i.e., the scoop for our work).The total force and total torque on the scoop are defined as

$$\mathbf{F} = \sum \mathbf{F_i}, \quad (2)$$

$$\mathbf{T} = \sum \mathbf{r_i} \times \mathbf{F_i}, \quad (3)$$

where $\mathbf{r_i}$ is the vector from the geometry's center of mass to the center of the ith facet element of the geometry and $\mathbf{F_i}$ is the force acting on it.

The high accuracy of DEM comes at the cost of long computation time. Hence it is not possible to run the DEM simulation real time within the OceanWATERS Gazebo simulation. Instead, the problem must be implemented off-line and force/torque results registered in a lookup table that includes a wide range of test cases, which may then be referenced by the Gazebo simulation. Although computation time cannot be decreased to real-time needs, it can be optimized in order to run the number of simulation on a single high performance desktop computer in a reasonable amount of time. Reduction of computation time is done primarily by increasing the simulation time step. In DEM applications, the time step is usually selected as a fraction (usually between 0.2 to 0.3) of the Rayleigh time step t_R, defined as [21]

$$t_R = \frac{\pi R_{min}}{c_R}, \quad (4)$$

Table 1. Key events: times and speeds

Event	Speed	Start time (s)
Terrain Approach	0.14 m/s	1.8
First Rotation	90 deg/s	2
Linear Translation	0.3 m/s	3
Second Rotation	90 deg/s	4

where c_R is a factor proportional to the shear modulus and R_{min} is the minimum particle radius. Equation 4, shows that the time step decreases when the shear modulus increases or the minimum particle radius decreases. Studies suggest that values above 1e+6 Pa do not significantly affect simulation results, even when the actual material shear modulus is higher [22]. Since the limitations with shear modulus are well understood, we focus on minimizing particle radius in the simulation. In order to minimize computation time and generate a lookup table of forces and torques for the OceanWATERS Gazebo framework, four analyses were performed. The first analysis aims at determining the largest single-sphere snow particle size to be used in the lookup table simulations. The second analysis, is focused on optimizing the geometric complexity of the ice crystal through the use of multi-spherical particles. The third study consists of analyzing data from the set of simulations run using the optimized particles for snow and ice. The same data is used to build the lookup table of forces and torques on the scoop to be integrated in the OceanWATERS Gazebo framework. The final analysis compares a representative simulation to experimental results with a scoop in a sand testbed to demonstrate the reliability of the EDEM simulation environment.

Particle Size of Snow-like Material

Since bulk snow particles are very small, they are impractical to implement in terms of computation time. Thus, the aim of this analysis is to identify the largest particle size that closely represents the bulk behavior of smaller particles. This avoids unnecessary reduction of the particle size without affecting the force and torque analysis results. To do so, the circular-linear-circular scoop trajectory described in Section 3 has been simulated using spheres of decreasing size with the parameters given in Table 1. The set S, described in Equation 5, lists the sphere diameters adopted in each simulation:

$$S = \{S_2, S_{2.5}, S_{3.25}, S_4, S_{5.25}, S_{6.5}, S_{8.25}, S_{10}\}. \quad (5)$$

where, for S_d, d is the diameter given in mm.

Table 2 lists the simulation parameters, including the terrain properties and interaction coefficients. In order to understand how different particle sizes influence the force and torque seen by the scoop, the magnitude of the force and torque from each simulation were compared, and can be seen in Figure 3. The data represented here is not smoothed to highlight how larger particles cause more fluctuation in the curve. The fluctuations decrease when the particle size decreases, until the two trends converge to the smoothest one, corresponding to Ø 2 mm. Observing the trends, it is noticeable how the force and torque magnitude decreases as the particle diameter decreases. In Figure 3, the Ø 5.25 mm trend presents few anomalous spikes of high magnitude which might be due to particles jamming during the scoop motion. Figure 4 is a 3D representation of Figure 3, where the data has been smoothed to easily visualize it. This figure shows more clearly that as the particle size decreases, the curves approach the Ø 2 mm

Table 2. Simulation parameters

Parameter	Value
Poisson's Ratio	0.36
Shear Modulus (Pa)	1e+7
Rolling Friction	0.05
Static Friction	0.58
Coefficient of Restitution	0.88
Solid Density (g/cm^3)	0.9167
Terrain Model	Elastic, non-cohesive
Gravity (m/s^2)	1.3

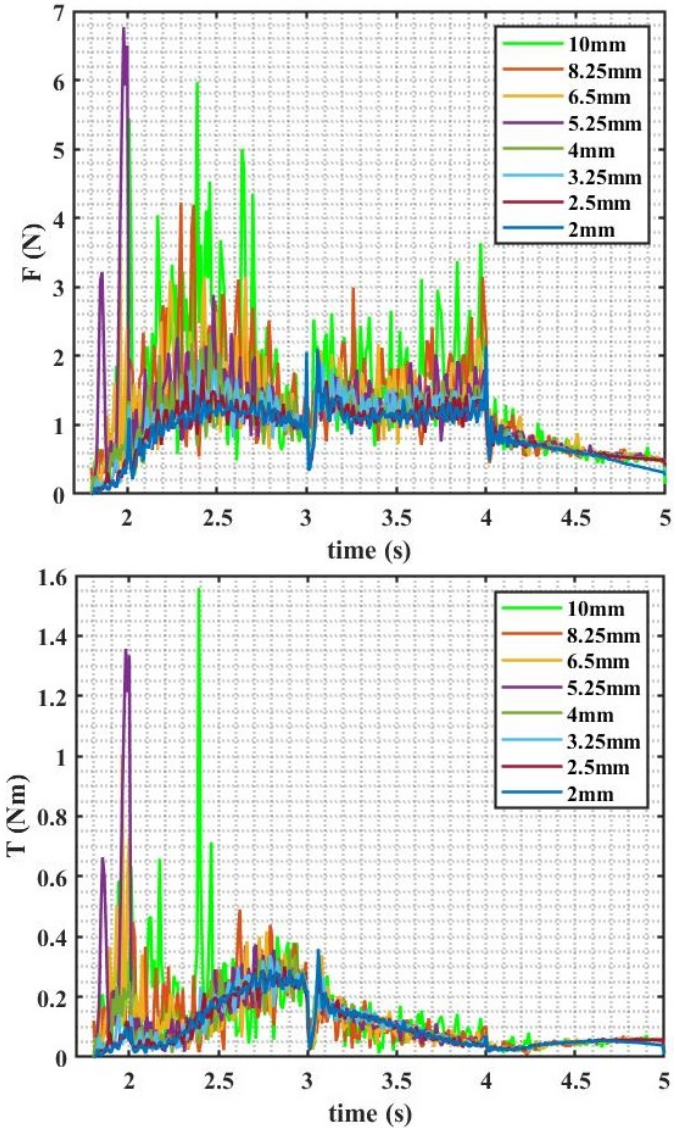

Figure 3. The top graph shows the magnitude of the force feedback applied on the scoop while traversing a bed of particles using the trajectory described in Section 2. The bottom graph shows the torque applied relative to the center of mass. The spikes are anomalies of the simulation. Some jamming of the material is likely to cause this behavior. This happens mainly on larger particle size.

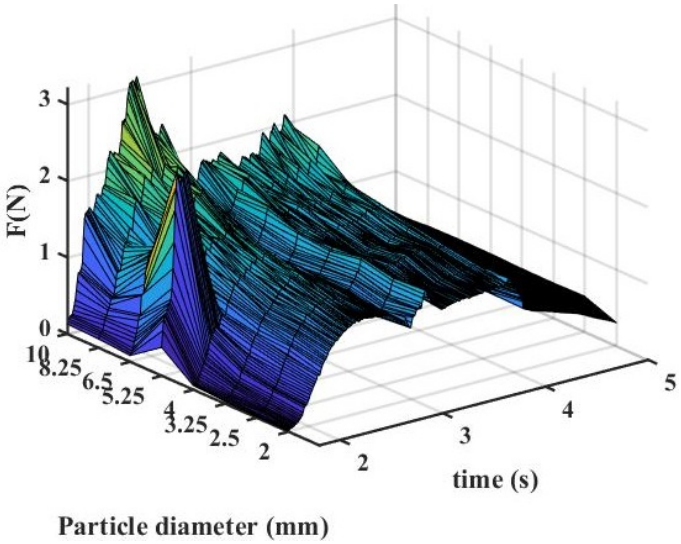

Figure 4. 3D plot of the force feedback as a function of time and particle diameter. It shows a convergence of the forces to a steady state as the particle size decreases. The spike appearing at 5.25 mm is likely due to a simulation anomaly.

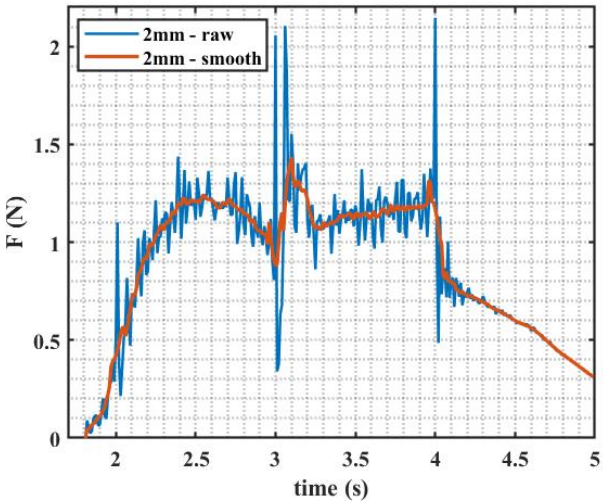

Figure 5. The graph shows the smoothed vs raw data for the simulation using Ø 2 mm particles.

trend, which has its raw and smoothed data trends highlighted in Figure 5. From Figure 4 it is visible that from 10 mm to 4 mm the trends experience a significant increase in force due to the larger particle size. Observing particles under 4 mm, the trends in force look similar. In order to estimate an optimized particle size, a tolerance of 20% to the variation in force and torque observed by each particle diameter is applied. A tolerance of 20% was chosen to reduce the overall computation time while maintaining a reasonable accuracy in the force and torque responses. To find the optimized particle size, first the maximum value of the smoothed force magnitude is isolated. Then, the maximum percent error

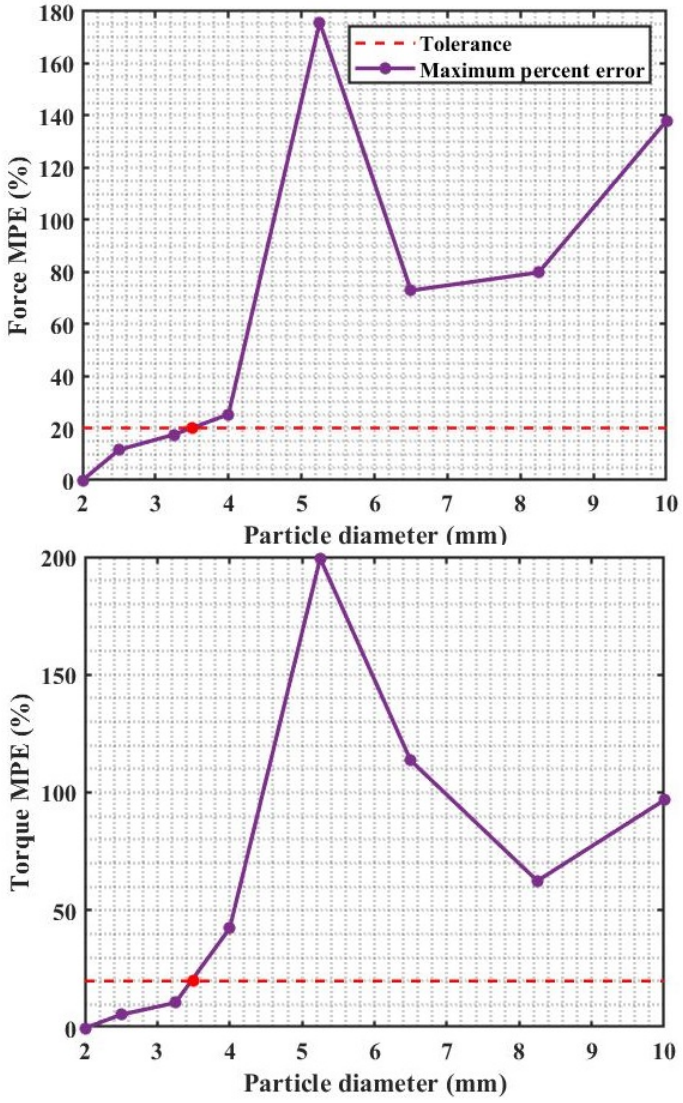

Figure 6. The two graphs show the average force (top) and torque (bottom) magnitude variation (MPE) as the particle size varies. The red dotted line is the threshold used to select the particle size.

(MPE) is calculated as:

$$MPE(S_d) = \frac{\max(\{S_d(0),\ldots,S_d(n)\}) - \max(\{S_2(0),\ldots,S_2(n)\})}{\max(\{S_2(0),\ldots,S_2(n)\})} 100. \quad (6)$$

Thus, the optimal particle size can be found with

$$S_{d,20\%} : MPE(S_d) \leq 20\%, \quad (7)$$

where $S_{d,20\%}$ represents the desired size. Figure 6 shows the maximum percent error for each particle diameter as purple dots, and the tolerance as a dashed red line. From the figure, it can be seen that the optimal particle diameter is given as Ø 3.5 mm, indicated as a red dot in the plot. In light of this result, the particle size chosen for simulations adopting snow as bulk material is a single sphere having diameter equal to Ø 3.5 mm.

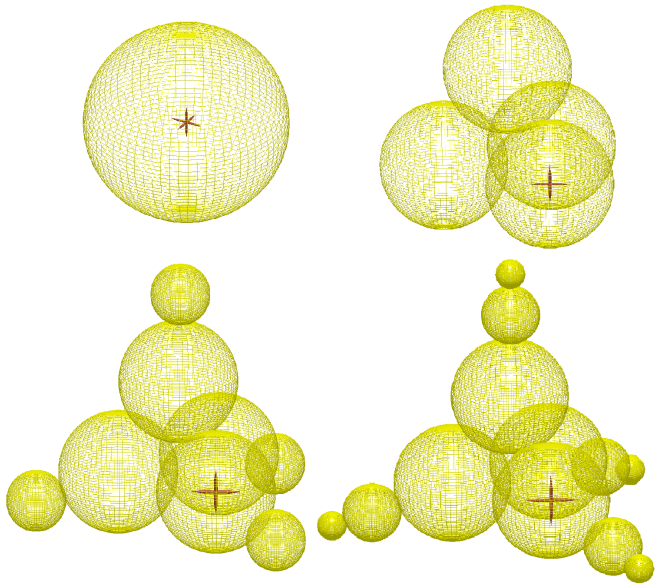

Figure 7. Approximations of tetrahedral particle with spheres in order of complexity: one sphere (upper-left), four spheres (upper-right), eight spheres (bottom-left), twelve spheres (bottom-right).

Shape Complexity of Ice-like Material

The second bulk material considered in this work consists of ice fragments. Although crushed ice particles may have disparate sharp configurations, it is here assumed that ice fragments have tetrahedral shape, which enable the particles to interlock together similar to actual ice. In DEM simulations, every particle shape is approximated using multi-sphere particles. The more accurate the spherical approximation, the smaller the minimum sphere radius R_{min}, which increases the computation time according to Equation 4. In this analysis four approximations of the tetrahedral ice particles are compared with respect to their resultant respective force magnitude trends on the scoop and the computation time. Simulation parameters for this analysis are the ones given in Tables 1 and 2. Given a regular tetrahedron of side 10 mm, the four considered approximations are shown in Figure 7. This size of tetrahedron was chosen such that the resulting particles would have diameters on the order of the diameter found for the snow-like particle. The simplest configuration is an inscribed sphere with a Ø 4 mm in the tetrahedron, shown in the top left of Figure 7. The top right configuration is a composition of four spheres having Ø 3.5 mm. The bottom left composition includes a further level of complexity, introducing four more spheres of Ø 1.75 mm at the corners. The best approximation of the tetrahedron is given in the bottom right corner where four more spheres of Ø 0.875 mm have been added to resemble the sharp polyhedron corners. The force magnitude trends, both raw (thin line) and smoothed (thick line), obtained from running the given scenario for each of the four particle configurations, are given in Figure 8 and the computation times are listed in Table 3. From Figure 8, it can be seen that the magnitude of the required force increases with particle complexity. This behavior can be explained by the fact that sharp particles have multiple contact points with the scoop and other particles. As a result, particles tend to interlock with each other and with the scoop, requiring a greater effort during the scooping process. This behavior is confirmed by the larger irregularities observed as the particle shape becomes more complex. Conversely, low fluctuations

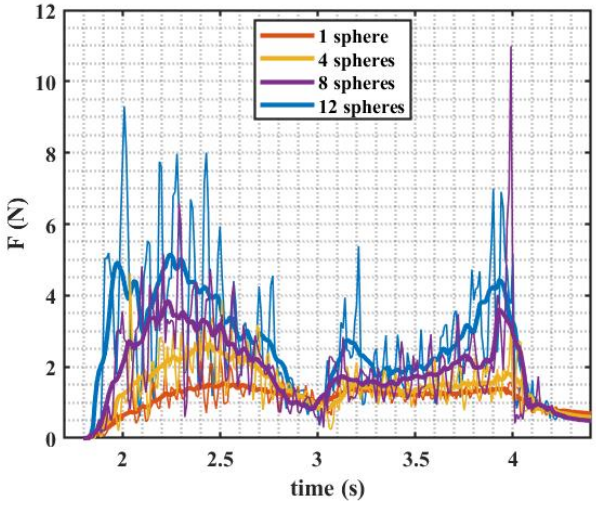

Figure 8. Force magnitude trend for the four particles of increasing complexity.

Table 3. Simulation time for particles with increasing complexity.

Configuration	Computation time (hours)
1 sphere	2.25
4 spheres	2.3
8 spheres	5
12 spheres	33

and low force magnitudes characterize the smooth behavior of single sphere particles, which allow for a more fluid scoop motion in the bulk material. The choice of the particle type in the present study was heavily driven by computation time optimization requirements. Hence, the 4-sphere configuration has been selected for ice simulations knowing that the actual force acting on the scoop can reach greater values.

Simulation Set for OceanWATERS Lookup Table

The previous analysis have established that the scooping strategy will be simulated using a Ø 3.5 mm single sphere for snow, and a clump of 4 spheres emulating a tetrahedron for ice fragments. The data presented in this section has been included in the OceanWATERS lookup table. Table 4 defines the scoop trajectory parameters used and Table 5 summarizes the set of simulations performed to fill the look-up table. For each bulk material type (ice and snow) and each bite depth one sample collection through 5 consecutive passes has been simulated in EDEM. Simulation parameters are summarized in Table 6. Furthermore, the data of each simulation has been smoothed to help visualization.

Table 4. Key event times and speeds

Event	Speed	Total Angle/Distance
First Rotation	30 deg/s	90 deg
Linear Translation	0.1 m/s	0.3 m
Second Rotation	30 deg/s	90 deg

Table 5. Values of simulation variables used in the lookup table simulation set.

Variable	Cases
Bulk Material - m	Ice, snow
Bite depth - d (mm)	15, 9, 5, 3
Pass - p	1,2,3,4,5

Table 6. Terrain parameters for lookup table simulation

Parameter	Value
Poisson's Ratio	0.36
Shear Modulus (Pa)	1e+7
Rolling Friction	0.05
Static Friction	0.58
Coefficient of Restitution	0.88
Solid Density (g/cm^3)	0.9 (ice) - 0.3 (snow)
Terrain Model	Elastic, non-cohesive

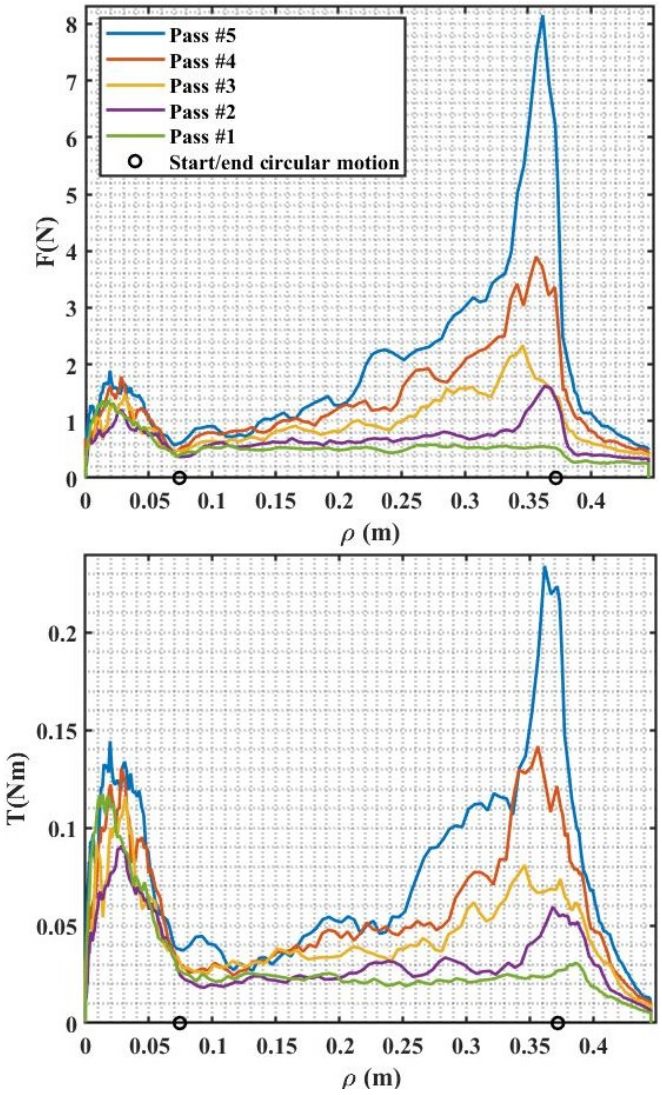

Figure 9. Comparison of force (above) and torque (below) magnitude resulting from subsequent 15mm bite depth passes for ice vs the horizontal scoop displacement.

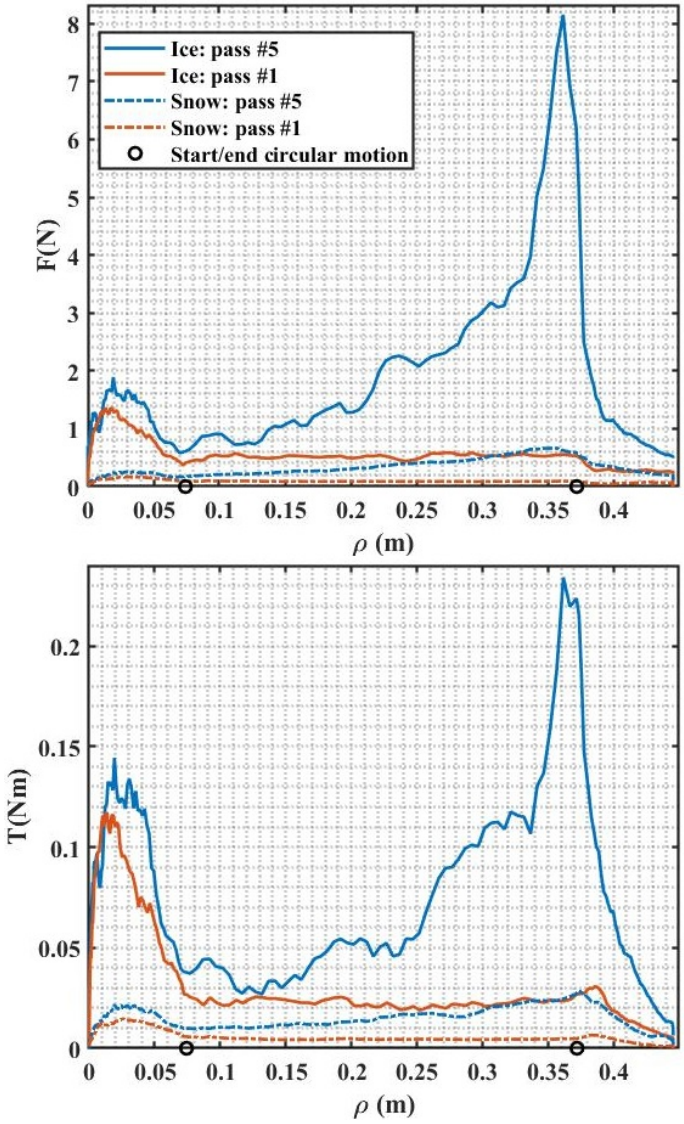

Figure 10. Comparison between force (top) and torque (bottom) magnitude from first and fifth 15 mm scooping pass for ice and snow vs the horizontal scoop displacement.

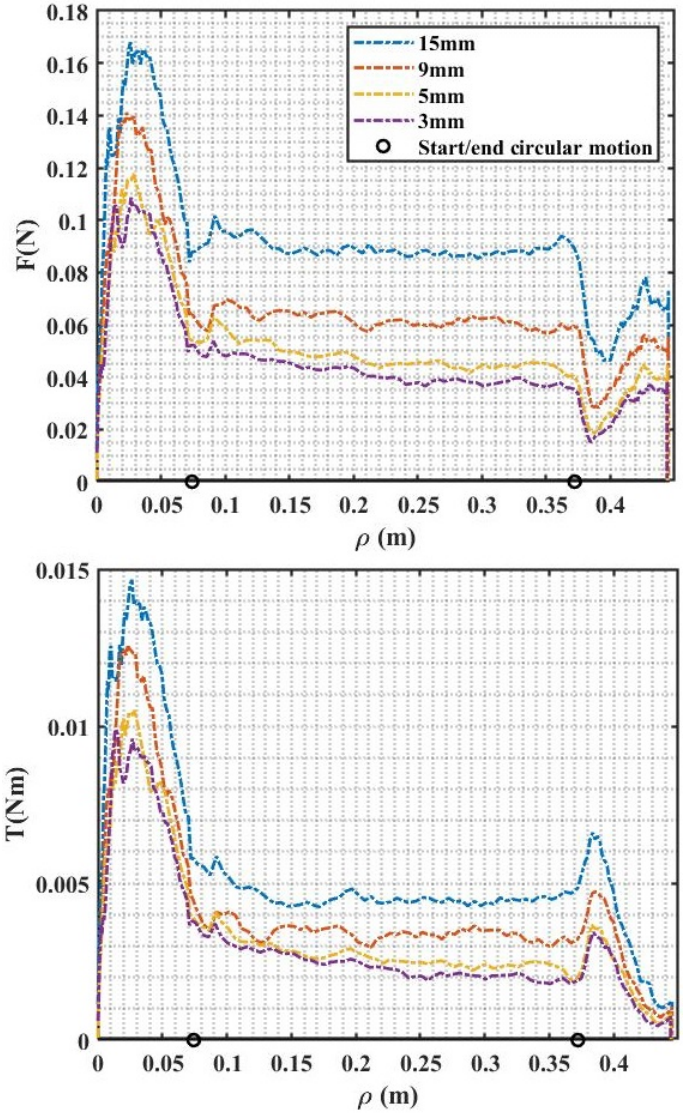

Figure 11. Comparison of force (above) and torque (below) magnitude for 15mm, 9mm, 5mm, 3mm bite depths, first pass, for snow vs horizontal scoop displacement.

Figure 9 represents the force and torque magnitude trends, with ice fragments as bulk material, as a function of the covered space along the trenching direction ρ when the bite depth is 15mm. The black circles on the ρ-axis defines the circular-linear and linear-circular transitions. The difference between passes is negligible during the first circular motion. Once the linear motion starts, the force follows an approximately linear change. The higher the pass number, the greater the increase in force, until the trend reaches a peak in correspondence with the start of the second circular motion. Recalling that an increase in pass number means increasing the depth, a greater slope in force for deeper trenching is justified by accumulation of bulk material in and in front of the scoop. A comparison of the force and torque applied to the scoop for the 1st and 5th pass of a simulation with a bite depth of 15 mm is shown in Figure 10. Figure 10 confirms what has been observed in Figure 8 regarding the fact that complex particles exert a higher force on the scoop than simple spheres, which is further enhanced by the difference in density of the bulk material. As a result, the force feedback registered from scooping in ice fragments is one order of magnitude larger than scooping in snow. The force and torque observed by the scoop operating in snow is given in Figure 11. Here the pass number is fixed at 1 and the bite depth varies. It can be observed that as bite depth increases, so does the force and torque applied to the scoop. Given the small bite depth during the first pass, there is no significant accumulation of bulk material in the scoop during the linear motion. While the scoop moves linearly, forces on the scoop either remain constant or decrease because the particles have not yet reached the back wall of the scoop (i.e., while the scoop translates, particles enter the cavity without hitting any scoop's surface). When the second circular motion starts, the change of attitude of the scoop causes particles to be pushed towards the bottom of the scoop causing an initial decrease in force followed by an increase as the bulk material hits the back scoop wall. Figures 9-11 present an initial peak in the middle of the first circular motion. This is due to the fact that

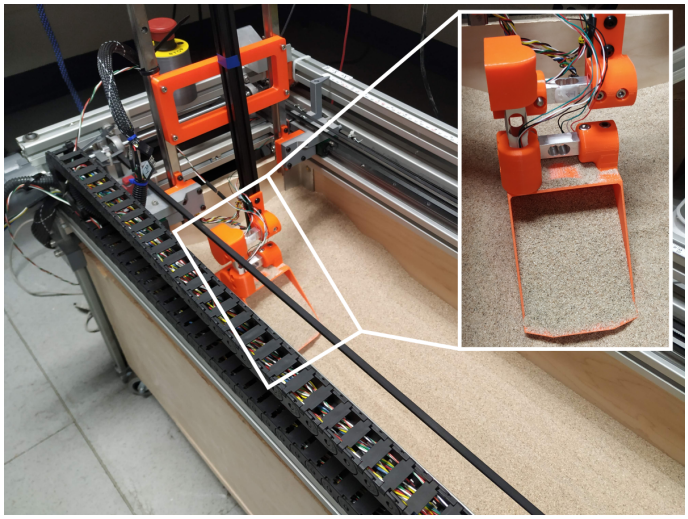

Figure 12. Data validation sand testbed: the 3D-printed scoop is mounted on a rail that allows for linear horizontal motion. Three load cells allow measurement of forces in the body frame directions.

front blade of the scoop submerges into the bulk material at higher depths than the given bite depth while performing the circular motion penetrating the terrain. The deepest point of blade submersion happens halfway through the rotation and corresponds to the initial peak.

Experimental Environment Validation

In parallel to the OceanWATERS virtual simulation under development at NASA Ames Research Center, a physical testbed is being developed at NASA JPL. Together both testbeds will validate lander autonomy strategies. As a first pass at validating the reliability of our own virtual simulation results, a simple experiment has been run using a sand testbed at NASA Ames. Figure 12 shows the testbed arrangement. After being manually inserted into the sand bed, the 3D-printed scoop model moves with a linear constant velocity of 0.01 m/s parallel along the rail to which it is attached. The scoop is equipped with three load cells each mounted orthogonal to one another in order to capture the entire force vector acting on the scoop. The scoop material is PETG. The top plot of Figure 13 shows the three force components in the scoop body frame resulting from the experiment. The same experiment was performed five times. The shadowed region surrounding each plot represents the 95% confidence interval while the dashed line represents the average value. The bottom plot in Figure 13 reports the force components obtaining replicating the testbed scenario on the EDEM simulation tool. Experimental force trends show an initial peak due to the fact that the scoop has been inserted manually in the sand, which exerts initial unwanted forces on the scoop. Proceeding with its linear motion, experimental forces assume values which are very close to the experimental ones. It can be seen from Figure 13 that forces from the physical experiment increase in magnitude more rapidly than in the simulation. This can be explained considering that the scoop and the test rig are not perfectly rigid, as it is assumed in the simulation. In reality, the scoop system responds to a force in the y direction bending towards the force direction, collecting more sand than calculated in the simulation. To a greater accumulation of bulk material corresponds a greater force in both the y and z direction, which again causes further bending of the system. The result is a greater increase in force in the testbed

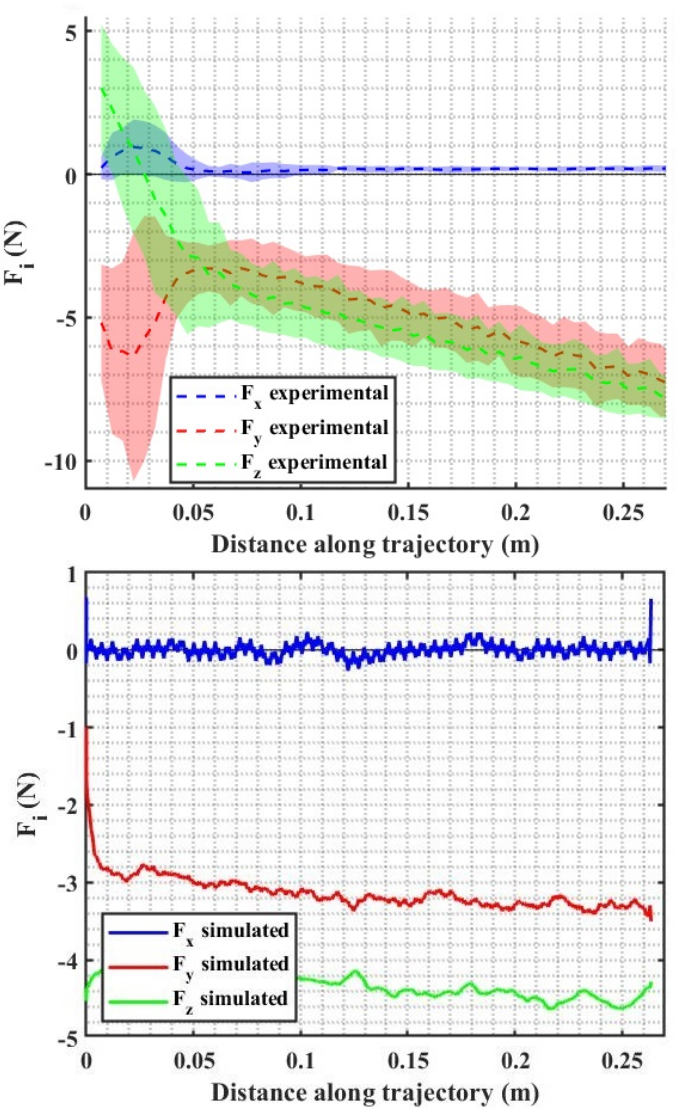

Figure 13. Comparison of the X, Y & Z force components acting on the scoop in the experimental test rig (top) and in the DEM simulation (bottom).

case compared to the simulation case, as observed in Figure 13. This experiment does not constitute a full validation of the interaction model. The final validation will be conducted in collaboration with JPL on their testbed. This experiment serves to inform the team in Ames on the reliability of the force values in terms of sign and order of magnitude.

5. Conclusions

This paper presented part of the Ocean Worlds Autonomy Testbed for Exploration Research and Simulation (OceanWATERS) simulator for future planetary exploration targeted at ocean worlds. The work belongs to a larger effort of simulating a lander platform in its realistic environment, targeted at autonomous science mission design. This paper focuses particularly on the interaction between the scoop end effector and icy granular material. The expected icy surface terrain composition and structure were discussed in Section 2. The different forms of icy materials expected on those worlds were described and their properties reviewed,

in order to inform on the assumptions that can be made to realistically simulate the terrain-scoop interaction. Two materials resembling snow and crushed ice were selected for the simulation in order to cover a range of properties. Section 3 described the trenching strategy, which is to collect the sample though multiple passes, referred as bites, with a scoop. The scoop approaches the terrain with a circular motion, moves with linear velocity parallel to the terrain to collect material and, with a second circular motion, leaves the soil. Targeted discrete element method (DEM) analyses allow for realistic simulation of the scoop-soil interaction in terms of forces and torques acting on the end effector. The EDEM software has been adopted as the DEM simulation tool. The key parameters of particle size and the particle shape complexity are explored to find a good trade off between simulation time and accuracy. With the resulting optimized size of Ø 3.5 mm particle and the chosen multi-sphere tetrahedron particle configuration, a set of simulations was run to create a lookup table that will be used to inform the OceanWATERS Gazebo simulator of the expected force feedback from the terrain for the given end effector trajectory. Finally, some preliminary validation of the DEM simulation was presented. The validation showed a similar trend, sign and order of magnitude in the force feedback through the trenching trajectory. However, due to the lack of rigidity of the real system compared to the ideal simulated case, forces on the scoop increase more rapidly in the experiment than in the simulation. Future research will explore other particle shapes and material properties. A look at bonded particles will also be explored. The experimental testbed will be equipped with motors that will allow circular motion of the scoop, allowing to simulate the entire scooping strategy. The final data validation will be conducted in collaboration with NASA JPL. In terms of the terrain research, breakable bonds will be added between adjacent discrete elements to simulate sintered ice grains. The strength between these bonds can be varied with depth to produce different desired strength gradients. Furthermore, different terrain geometries and trenching trajectories will be explored.

ACKNOWLEDGMENTS

Thanks NASA Ames Research Center & the Intelligent Robotics Group (IRG) for providing the testing facilities required for this work. Thanks to the OceanWATERS team and the principal investigator Larry Edwards for the support. Thanks Loic Tissot-Daguette for providing the physical testbed to prove the forces on the scoop. The work of J. C. Case was supported by a NASA Space Technology Research Fellowship (NSTRF) (NNX15AQ75H).

REFERENCES

[1] NASA, "Ocean worlds, water in the solar system and beyond," last accessed 16 October 2019. [Online]. Available: https://www.nasa.gov/specials/ocean-worlds/

[2] G. McCartney, "New organic compounds found in enceladus ice grains," 2019, last accessed 16 October 2019. [Online]. Available: https://www.jpl.nasa.gov/news/news.php?feature=7510

[3] S. S. Grace Tan-Wang, "Europa lander mission concept overview," 2019, last accessed 16 October 2019. [Online]. Available: https://www.jpl.nasa.gov/missions/web/absscicon/02-AbsSciCon-Mission-Overview-13Jun2019-no-BU.pdf

[4] M. Allan, "Planetary rover simulation for lunar exploration missions," *IEEE Aerospace Conference*, 2019.

[5] M. Quigley, "Ros: an open-source robot operating system," *ICRA*, 2009.

[6] S. Gorevan, "The rock abrasion tool on the mars exploration rovers," last accessed 16 October 2019. [Online]. Available: https://mars.nasa.gov/mer/mission/instruments/rat/

[7] N. JPL, "Msl, sampling system," last accessed 16 October 2019. [Online]. Available: https://msl-scicorner.jpl.nasa.gov/samplingsystem/

[8] R. G. Bonitz, "Nasa mars 2007 phoenix lander robotic arm and icy soil acquisition device," *Journal of Geophysics Research*, 2008.

[9] C. A. Gallo, "Comparison of isru excavation system model blade force methodology and experimental results," 2010.

[10] R. Greeley and R. Sullivan, "Terrestrial sea ice morphology: Considerations for europa," *ICARUS*, 1998.

[11] L. Jing, *Fundamentals of Discrete Element Methods for Rock Engineering: Theory and Applications*, 2007.

[12] "Edem simulation," last accessed 16 October 2019. [Online]. Available: https://www.edemsimulation.com/

[13] J. Saur, S. Duling, L. Roth, X. Jia, D. F. Strobel, P. D. Feldman, U. R. Christensen, K. D. Retherford, M. A. McGrath, F. Musacchio *et al.*, "The search for a subsurface ocean in ganymede with hubble space telescope observations of its auroral ovals," *Journal of Geophysical Research: Space Physics*, vol. 120, no. 3, pp. 1715–1737, 2015.

[14] K. Hand, A. Murray, J. Garvin, W. Brinckerhoff, B. Christner, K. Edgett, B. Ehlmann, C. German, A. Hayes, T. Hoehler *et al.*, "Europa lander study 2016 report: Europa lander mission," *NASA Jet Propuls. Lab., La Cañada Flintridge, CA, USA, Tech. Rep. JPL D-97667*, 2017.

[15] W. C. J. D. G. H. R. H. R. J. T. M. M. M. Carlson, RW, "Europa's surface composition," in *Europa*. University of Arizona Press Tucson, 2009, pp. 283–327.

[16] J. M. Moore, G. Black, B. Buratti, C. B. Phillips, J. Spencer, and R. Sullivan, "Surface properties, regolith, and landscape degradation," in *Europa*. University of Arizona Press Tucson, 2009, pp. 329–349.

[17] D. E. Hobley, J. M. Moore, A. D. Howard, and O. M. Umurhan, "Formation of metre-scale bladed roughness on europa's surface by ablation of ice," *Nature Geoscience*, vol. 11, no. 12, p. 901, 2018.

[18] G. B. Hansen and T. B. McCord, "Amorphous and crystalline ice on the galilean satellites: A balance between thermal and radiolytic processes," *Journal of Geophysical Research: Planets*, vol. 109, no. E1, 2004.

[19] J. L. Molaro, M. Choukroun, C. B. Phillips, E. S. Phelps, R. Hodyss, K. L. Mitchell, J. M. Lora, and G. Meirion-Griffith, "The microstructural evolution of water ice in the solar system through sintering," *Journal of Geophysical Research: Planets*, vol. 124, no. 2, pp. 243–277, 2019.

[20] R. Arvidson, R. Bonitz, M. Robinson, J. Carsten, R. Volpe, A. Trebi-Ollennu, M. Mellon, P. Chu, K. Davis, J. Wilson *et al.*, "Results from the mars phoenix lander robotic arm experiment," *Journal of Geophysical Research: Planets*, vol. 114, no. E1, 2009.

[21] Y. J. Huang, O. J. Nydal, and B. Yao, "Time step criterions for nonlinear dense packed granular materials in time-driven method simulations," *Powder technology*, vol. 253, pp. 80–88, 2014.

[22] EDEM, "Computation time considerations," last accessed 16 October 2019. [Online]. Available: https://www.edemsimulation.com/blog-and-news/blog/particle-shear-modulus-it-can-save-you-time/

BIOGRAPHY

Damiana Catanoso *received her B.S. degree in Aerospace Engineering from La Sapienza University of Rome in 2015 and a double M.S degree in Space Automation and Control from the University of Wuerzburg and Lulea University of Technology in 2019. Her work focuses on guidance navigation and control of small satellites flying in formation and interplanetary robotics systems.*

Thomas Stucky *received two B.S. degrees in Physics and Applied Mathematics from the University of Utah in 2015. He is currently a systems developer in the Carl Sagan Center for the Study of Life in the Universe at the SETI Institute. His interests are robot autonomy and computational physics to solve problems related to autonomy.*

Jennifer Case *received a B.S. in mechanical engineering with an emphasis in mechatronics from Northern Illinois University in 2013 and M.S and Ph.D degrees in mechanical engineering from Purdue University in 2019. Her work focuses on enabling control of highly deformable robots.*

Arno Rogg *received a B.S. & M.S. in microengineering from the Swiss Institute of Technology of Lausanne (EPFL) in 2016. He is currently working at NASA Ames Research Center in the Intelligent Robotics Group. His work focuses on planetary exploration, high reliability robotic systems and rover research & development with a focus on autonomous systems & rover mobility.*